

Elasticity of Poly(diacetylene) Gels: Measurements by Electric Field Coupling

A. Kapitulnik, K. C. Lim, S. A. Casalnuovo, and A. J. Heeger*

Institute for Polymers and Organic Solids, Department of Physics, University of California, Santa Barbara, Santa Barbara, California 93106. Received July 15, 1985

ABSTRACT: We present a comprehensive description of our studies of the elastic properties of gels of poly(diacetylene)-4BCMU in toluene. The experimental results utilize the acoustobirefringence technique with excitation of elastic modes via electric field coupling to the anisotropic rodlike molecules which make up the gel network. A theory of this electric field coupling to elastic modes is developed and compared with the experimental results. The shear modulus (and its dependence on the polymer network concentration) is obtained either from resonance excitation of transverse modes or from oscillatory transient decay of these underdamped modes. These techniques have been used to measure shear wave sound velocities as low as a few centimeters per second for polymer concentrations near the critical value. The concentration dependence of the elastic modulus, $\mu(c) \sim c^{2.9}$, is discussed in terms of a gel made of a network of rods connected by semiflexible joints.

I. Introduction

The discovery¹ that, with proper choice of side groups, macromolecules of poly(diacetylene) can be dissolved in simple solvents opened the way for extensive experimental studies designed to probe the effects of changes in polymer conformation on the delocalized (conjugated) electronic structure.¹⁻⁵ Solutions of poly(diacetylene) macromolecules were found to exhibit dramatic color change transitions when the solvent/nonsolvent ratio or the temperature was varied.¹⁻⁵ Patel et al.¹ argued that these color changes resulted from a planar-nonplanar conformational transition of the poly(diacetylene) macromolecules in dilute solution. Direct evidence of the conformational transition came from the light scattering and birefringence studies of Lim et al.^{3,4} which demonstrated a major change in hydrodynamic radius coincident with the spectroscopically observed transition. They interpreted their results in terms of a reversible rod-coil transition and showed that in the dilute limit the measured diffusion constants were concentration independent, indicative of a single-chain phenomenon. For poly(diacetylene)-4BCMU (where the side group is $R = 4BCMU = (CH_2)_4OCONHCH_2COOC_4H_9$) dissolved in toluene, the polymer has a coil conformation and the solution is yellow above $\sim 70^\circ\text{C}$. At lower temperatures, the conformation is rodlike, and the solution is red.

In the absence of attractive interactions, a solution of rodlike macromolecules would be expected to exhibit a liquid crystalline phase for concentrations $C > C_0 \simeq (L^2d)^{-1}$, where L and d are the length and diameter, respectively, of the rod.⁶ The possibility of "gelation" of polymer rods in solution was discussed by Doi and Edwards⁷ and by Doi and Kazuu.⁸ They ignored the potential for nematic ordering and considered the elastic properties of a network of rods with hard-core repulsive interactions only. As noted by Doi and Kazuu⁸ such a network is, however, not truly a gel; at low enough frequencies there would be no elastic restoring force of a network of non-bonded rods to a shear deformation.

Gelation requires an attractive interaction,⁹ a chemical bond, between the polymers which make up the network. Many studies have been described on isotropic gels in which the attractive interaction takes the form of a permanent covalent bond. Weaker, reversible gelation can be expected if the attractive interaction is due to hydrogen bonding or to van der Waals dispersion forces. Reversible gelation has been reported and described¹⁰ for poly(diacetylene)-4BCMU. These studies demonstrated that for gelation to occur, the macromolecules must be in the rod

conformation; to the accuracy of the experiment the gel-sol transition and the rod-coil transition are coincident.

For poly(diacetylene)-4BCMU, both intermolecular hydrogen bonding and van der Waals interactions can contribute to the net attractive interaction. Intramolecular hydrogen bonding (between successive side chains) is known to be important and to contribute to the stiffness of the rod conformation.¹ The analogous intermolecular hydrogen bonding (between side chains on different molecules) would be expected to tend to link molecules into a network. On the other hand, gelation has been reported for poly(diacetylene) molecules with side chains that do not have hydrogen bonding.¹¹ Moreover, the absence of gels in the coil phase, even at concentrations more than 2 orders of magnitude greater than C_* (at which the coils start to overlap) where the density of open hydrogen bonds is high, argues that this may not be the dominant intermolecular interaction. The existence of a highly polarizable π -electron system implies a relatively strong short-ranged van der Waals interaction. The combination of these two leads to a net intermolecular attractive interaction which is sufficient to cause gelation.¹⁰

The two features which characterize the poly(diacetylene) system, rodlike molecules with high rigidity and a moderate attractive interaction, should lead to a rather general effect expected for all polymers having these properties: anisotropic gelation. In other words, gels made up from networks of such macromolecules might be expected to exhibit remanent nematic alignment, i.e., nematic gels.^{12,13}

As a result of the π -electron delocalization along the backbone, the poly(diacetylene)-4BCMU macromolecules have a large electronic polarizability parallel to the chain direction ($\alpha_{\parallel} \sim 10^{-18} \text{ cm}^3$), and they are highly anisotropic: $\alpha_{\perp}/\alpha_{\parallel} \ll 1$. Thus, even in cases where there is no remanent nematic order (macroscopically isotropic) the anisotropy of the conjugated rodlike molecules causes them to align along the direction of a low-frequency electric field. Although this tendency is opposed by the elastic restoring forces of the gel network, such alternating electric fields can induce resonant deformation and thereby lead to resonant birefringence in the gel. Since $(\alpha_{\parallel} - \alpha_{\perp}) \sim \alpha_{\parallel}$ is large, the deformation-induced birefringence is large and relatively easy to detect. This technique was used in an earlier publication to probe the elastic properties of gels of poly(diacetylene)-4BCMU in toluene.¹⁴

In this paper we present a comprehensive description of our studies of the elastic properties of gels of poly(diacetylene)-4BCMU in toluene. In section II, we give a

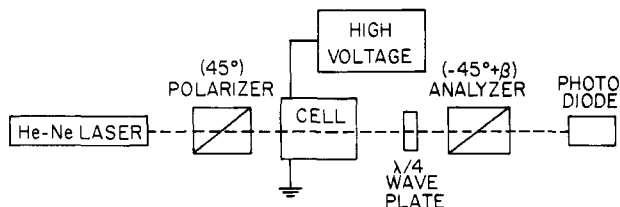


Figure 1. The birefringence experiment, indicating the basic optics.

detailed description of the acoustobirefringence technique. The theory of electric field coupling to the elastic modes in a gel made from anisotropic rods is developed in section III. The experimental results obtained by electric field coupling to the elastic modes of the gel are presented in section IV. Section V describes the use of the transient decay of the underdamped gel modes to obtain complementary data on the elasticity and on the viscous damping of the gel. This method is reported here for the first time as a means for studying the elastic properties of gels. A discussion of the principal conclusions is given in the final section.

II. Description of the Birefringence Experiment

The experimental configuration is typical for an electrooptic birefringence measurement.¹⁵ An electrooptic cell with a set of parallel electrodes was placed between Glan-Thompson crossed polarizers. The axes of the polarizer and the orthogonal analyzer were set at $\pi/4$ with respect to the electrodes so that the electric field was at $\pi/4$ with respect to both the polarizer and the analyzer. A 5-mW He-Ne laser beam ($\lambda = 6328 \text{ \AA}$) was incident through the first polarizer, through the electrooptic cell between the electrodes, then through a quarter-wave ($\lambda/4$) plate (when appropriate), and finally through the analyzer. The exit light intensity was monitored by a photodiode. The parallel electrodes were made of two thick aluminum plates spaced 5 mm apart; the electrodes defined an optical path length of 1 cm. Care was taken to eliminate stress birefringence in the windows of the electrooptic cell. With crossed polarizer and analyzer (and with no $\lambda/4$ plate) the signal from the photodiode in zero applied field resulting from light leakage etc. was below the noise level. Under these conditions, the detected signal⁵ is proportional to $(\Delta n)^2$, where $\Delta n = (n_{\parallel} - n_{\perp})$ is the difference between the parallel and perpendicular refractive indices of the medium with directions defined relative to the electric field. After the analyzer is rotated a small angle β (away from $\pi/2$ with respect to the polarizer) and a $\lambda/4$ plate is inserted, the photodiode signal is proportional to Δn .¹⁵

We report results of two different experiments, both of which utilize this same basic birefringence configuration. For the electric field coupling to the resonant elastic modes, we used the Δn configuration. For small β , the signal resulting from a phase shift δ in the medium is proportional to

$$\Delta I_{(t)} = I_0 \sin \delta \sin 2\beta \quad (1)$$

where

$$\delta = (2\pi t/\lambda)\Delta n \quad (2)$$

and t is the optical path length in the cell. All of the results presented in this paper were obtained under conditions such that any field-induced change in δ was small so that $\sin \delta \sim \delta$ and the signal is proportional to Δn . The same configuration (Δn) was used for the measurements of the underdamped decay of the elastic modes of the gel. In these measurements we neglected the extinction, which was in all cases very small compared to the measured intensities (for the most concentrated gel, $\sim 90\%$ of the incident beam was transmitted). For gels with relatively high concentrations the remanent nematic order caused the optical axis to rotate even in zero field. For such cases, we used the $\lambda/4$ plate to compensate the angle such that eq 1 is valid. A schematic diagram of the electrooptic birefringence instrumentation is given in Figure 1.

Electrophoresis usually occurred in the cell when the polymer was subjected to a constant electric field. This effect was used

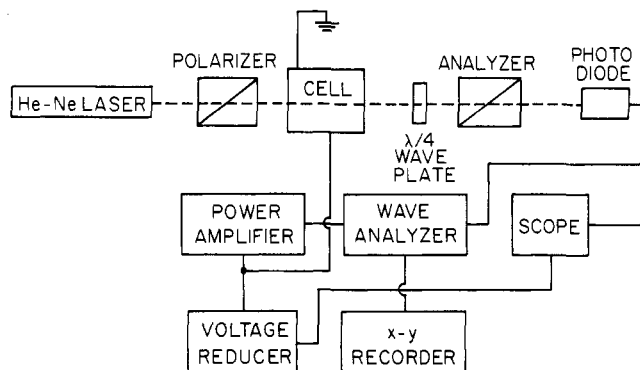


Figure 2. Block diagram of the resonance birefringence experiment (built around the basic optics in Figure 1).

to study long relaxation times in gels, involving large deviations from equilibrium. For studying the elastic properties, a low-frequency alternating field was applied. The output of a wave analyzer (HP) was amplified, passed through a high-vacuum relay switch, and connected to a 1:20 ratio step-up transformer. The high-voltage output of the transformer was connected directly to the electrodes of the electrooptic cell. This configuration was capable of generating a maximum-peak alternating electric field of several thousand volts/cm with a frequency range from 20 to $2 \times 10^3 \text{ Hz}$. The high-vacuum switch has a switching time of less than 5 ms. No "ringing" of the applied field was observed. The applied field across the electrodes was measured by using a 500:1 voltage divider and monitored directly on the oscilloscope. In this way the signal and applied ac field could be directly compared. For the empty electrooptic cell and for the cell filled with pure toluene, no birefringence signal was detectable even at the highest fields. The experimental setup is shown in more detail in Figure 2.

The poly(diacetylene)-4BCMU used in these experiments was obtained from T. Prusik of Allied Corp. This material has been previously characterized: the mean molecular weight corresponds to approximately 2400 diacetylene repeat units¹ with an end-to-end length of about $1.2 \mu\text{m}$. In our experiments the poly(4BCMU) was dissolved in toluene at $\sim 80^\circ\text{C}$. At this temperature, the solution is yellow, and the polymer molecules are in the coil configuration. The solution was allowed to cool through the conformational transition to room temperature. At room temperature the solution is red, characteristic of the extended rodlike conformation. Concentrations used ranged from $\sim 5 \times 10^{-4} \text{ g}$ to $\sim 5 \times 10^{-2} \text{ g/cm}^3$.

III. Electric Field Coupling to the Elastic Modes of the Gel: Theory

The equation of motion of a single rodlike molecule oriented at an angle θ with respect to an electric field, $E = E_0 \hat{Z} \cos \omega t$, is given as follows:

$$I \frac{d^2\theta}{dt^2} + (I/\tau) \frac{d\theta}{dt} + pE_0 \cos \omega t + \Delta\alpha E_0^2 \cos^2 \omega t \cos \theta \sin \theta = 0 \quad (3)$$

where I is the moment of inertia of the molecule, τ is the microscopic relaxation time, p is the permanent dipole moment, and $\Delta\alpha = (\alpha_{\parallel} - \alpha_{\perp})$ is the difference between the parallel and perpendicular polarizabilities. For a dilute solution of rods, τ is determined by Brownian motion and is directly related to the rotational diffusion constant.⁵ The mean molecular weight of the poly(diacetylene)-4BCMU corresponds to approximately 2400 monomer units, i.e., a length of $\sim 1.2 \mu\text{m}$ and a total mass of $M \sim 2 \times 10^{-18} \text{ g}$. Thus $I = ML^2/12 = 2.4 \times 10^{-27} \text{ g cm}^2$. Since the side-chain length is $\sim 25 \text{ \AA}$, the rodlike macromolecules are characterized by $L \simeq 1.2 \mu\text{m}$ and $d \simeq 50 \text{ \AA}$. Because of its symmetry, the ideal poly(diacetylene)-4BCMU will have no dipole moment. Although defects and imperfections could lead to permanent dipoles, field-induced birefringence measurements show that $p \leq 10^{-24} \text{ erg/(cm esu)}$.

Thus, for the moderate fields utilized in our experiments we can neglect any torque due to permanent dipoles. In the following paragraphs we use the microscopic equation for a single anisotropic rod to obtain the parameters in the elastic equations for a gel made up from a network of such molecules.

Polymer gels are two-component systems: a polymer network embedded in a solvent. Therefore, when treating a gel as a continuous medium, one must introduce a coupling between the elastic equation of the polymer network and the hydrodynamic equation of the solvent. This has usually been done via a Stokes term, proportioned to the relative velocity. We therefore write the equation of motion for the solvent (displacement \mathbf{u}_s)

$$\rho_s \ddot{\mathbf{u}}_s = \eta_0 \nabla^2 \mathbf{u}_s + \nabla P + \phi(\dot{\mathbf{u}}_n - \dot{\mathbf{u}}_s) \quad (4)$$

and for the network (displacement \mathbf{u}_n)

$$\rho_n \ddot{\mathbf{u}}_n = \mu \nabla^2 \mathbf{u}_n + (K + \mu/3) \nabla(\nabla \cdot \mathbf{u}_n) + \phi(\dot{\mathbf{u}}_s - \dot{\mathbf{u}}_n) + \mathbf{F}(E(t), \mathbf{u}_n) \quad (5)$$

where η_0 is the viscosity of the pure solvent, P is the pressure, ϕ is the friction coefficient between the network and the solvent, and K and μ are the bulk and shear moduli of the network, respectively. The external force \mathbf{F} derives from the interaction between the external electric field $E(t)$ and the network. For induced dipole moment we expect $|\mathbf{F}|$ to be proportional to $E^2(t)$. The determination of the dependence of \mathbf{F} on \mathbf{u}_n is more delicate and involves a proper averaging of the interaction.

Microscopically, each molecule is represented by a rod of length L attached to other rods. Thus, the microscopic stiffness of the network comes from a combination of bending the rods and bending the joints. If the mean distance between cross-links is a and the molecular diameter of the polymer is d , then the polymer concentration is given by

$$c \simeq d^2 a / a^3 = (d/a)^2 \quad (6)$$

The bending force constant of a rod of length a is

$$\chi_0 = b Y I / a^3 \quad (7)$$

where Y is the Young's modulus of the rod, I is the moment of inertia around the axis of the cross section, and b is a number dependent on the boundary conditions (typically $b \sim 10$). The shear modulus of such a network of rods (ignoring bending of the joints) is given by

$$\mu = \chi_0 a^{-1} = b Y I / a^4 = (b Y I / d^4) c^2 \quad (8)$$

Thus, for a network of rods of circular cross section (except for constants of order unity)

$$\mu \simeq Y c^2 \quad (9)$$

We shall discuss the c^2 dependence when analyzing the experimental data.

The elastic energy due to small deformation (bending) of the rod between joints i and $(i+1)$ is given by

$$U_0^i \simeq (1/2) \chi_0 (a \delta \theta_i)^2 \quad (10)$$

where $\delta \theta_i$ is a small change in the angle between the molecular axis and the electric field. The change in network energy resulting from the interaction with the electric field is

$$U_1^i = (1/2) \chi_1(t) (a \delta \theta_i)^2 \quad (11)$$

where $\chi_1(t)$ is an effective time-dependent force constant

$$\chi_1(t) = (\Delta \alpha E_0^2 / a^2) \cos^2 \omega t \quad (12)$$

assuming induced dipole moments only; see eq 4.

Let us consider the transverse component of eq 6 (since we are interested in the underdamped transverse modes found in the experimental results). If we denote by θ_0^i the angle between the i th molecular segment of length a and the direction of the field and by $\delta \theta_i$ the change in that angle due to applying the field, then the transverse component of \mathbf{F} is given by

$$F_t = \Delta \alpha E^2(t) \sum \cos(\theta_0^i - \delta \theta_i(t)) \sin[\theta_0^i - \delta \theta_i(t)] \quad (13)$$

where the sum is restricted to segments i which are part of the infinite cluster (denoted by Ω) per unit volume of the gel. For small fields, $\delta \theta_i$ is very small (more generally, $\delta \theta_i$ depends on θ_0^i) and we can expand eq 14 and make the small-angle approximation

$$F_t \simeq \Delta \alpha E^2(t) \sum_{i \in \Omega} [(1/2) \sin 2\theta_0^i + \delta \theta_i \cos 2\theta_0^i] \quad (14)$$

In order to get an expression which depends on network displacement vector, we must average eq 14 over the distribution function of the segments $f(\theta_0)$. Since we are dealing with induced dipole moments, $f(\theta_0) = f(\pi - \theta_0)$ for the rods have inversion symmetry. For long wavelengths where the motion is over a large number of molecules the torque on segments at θ_0 and at $(\pi - \theta_0)$ is equal; consequently $\delta \theta(\theta_0) = \delta \theta(\pi - \theta_0)$. As a result

$$\int_0^\pi \sin(2\theta) f(\theta) (2\pi \sin \theta) d\theta = 0 \quad (15a)$$

$$\int_0^\pi \delta \theta \cos(2\theta) f(\theta) (2\pi \sin \theta) d\theta \neq 0 \quad (15b)$$

so that eq 14 is reduced to

$$F_t \simeq \Delta \alpha E^2(t) \bar{\rho} \delta \theta \quad (16)$$

where $\bar{\rho}$ is the density of the gel network and $\delta \theta$ is the average field-induced angular displacement. This implies that F_t is proportional to the macroscopic network displacement \mathbf{u}_n . Note that for sufficiently small wavelengths, the demand that $\delta \theta(\theta_0) = \delta \theta(\pi - \theta_0)$ is no longer fulfilled (zigzag orientations are important when the wavelength begins to approach a). In this regime $\delta \theta(\theta_0)$ is an odd function of θ_0 , implying that F_t will be proportional to $\delta \theta^2$ (or u_n^2).

On the basis of the gel configuration described above, we can assume only shear modes in which the solvent and network move together. Thus setting $\mathbf{u}_s = \mathbf{u}_n$, we add eq 4 and 5 to obtain the following equation for the total transverse displacement, u :

$$\rho \ddot{u} + \eta \dot{u} + \mu \nabla^2 u + (K_1 \cos^2 \omega t) u = 0 \quad (17)$$

In eq 17, ρ is the density of the gel and η is an effective viscosity which depends on the wavelength as well as on ϕ . The final term in eq 17 is the external force due to the interaction of the network with the external electric field $E(t)$ (see eq 5). From eq 12 and 16, this force term takes the given form with K_1 proportional to E_0^2 . Taking the Fourier transform of eq 17, we obtain (using $\nabla^2 u_q = -q^2 u_q$)

$$\rho \ddot{u}(q) + \eta \dot{u}(q) + [K_0(q) - \frac{1}{2} K_1] [1 - s \cos 2\omega t] u(q) = 0 \quad (18)$$

where $s = K_1 / (2K_0 - K_1)$ and $K_0 = q^2 \mu$. Equation 18 describes a series of resonant normal modes. Provided $K_0 \gg K_1$, the parameter $s \ll 1$, so eq 18 yields a resonant response at frequencies

$$\omega_0(q) = (K_0(q) / \rho)^{1/2} = (\mu / \rho)^{1/2} q = v_s q \quad (19)$$

when driven parametrically at $\omega = \omega_0(q)$; v_s is the trans-

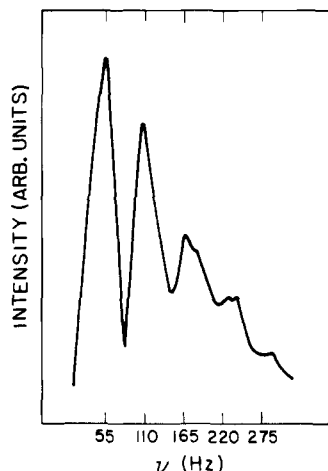


Figure 3. Resonance scan for a ~ 0.5 wt % poly(diacetylene) gel. The boundary conditions were zero displacement at the walls.

verse acoustic mode sound velocity of the gel.

The value of K_0 arises from the enumeration of all the contributions of the infinite cluster backbone to the stiffness of the network. Since isolated clusters and dangling bonds will not contribute either to the elastic stiffness (K_0) or to the electric field energy "stiffness" (since such disconnected pieces will simply reorient), we postulate that the ratio $K_1/K_0 = \chi_1/\chi_0$ (where χ_0 and χ_1 are given in eq 8 and 13), thereby relating the microscopic constants to those of the continuum limit. The ratio K_1/K_0 is therefore given by $\chi_1/\chi_0 \approx (\Delta\alpha E_0^2)/Yc^2a^3 = (\Delta\alpha E_0^2)a/Yd^4$; thus s can be estimated from the microscopic parameters. For concentrations above, but near, the gel point, $a \sim L/10 \approx 10^{-5}$ cm. Thus, for $E_0 \sim 10^3$ V/cm, $\Delta\alpha = 10^{18}$ cm³, and $Y \approx 10^7$ dyn/cm², one finds $\chi_0/\chi_1 \approx 10^{-3}$. At higher concentrations (as the gel becomes more stiff) the ratio is even smaller. Thus $s \ll 1$ except for concentrations so close to the gel point that $K_0 \rightarrow 0$.

We therefore conclude that in the gel, when applying an electric field, the dominant response for a transverse mode will be $\mu(t) \approx \cos(\omega_0 t)$. Harmonics will be observed but with much smaller amplitude (the n th harmonic, for example, will have a prefactor proportional to $S^n \ll 1$). Also any mixing in of longitudinal modes will scale with a high power of s . Thus, since the distortion $u(t)$ scales with $L\delta\theta$, the deformation-induced birefringence should exhibit resonance behavior when the frequency of the applied electric field is equal to $\omega_0(q)$.

IV. Electric Field Coupling to the Elastic Modes of the Gel: Experimental Results

The resonant deformation induced birefringence predicted in section III has been observed experimentally. Figure 3 shows a typical scan of the electric field induced birefringence in the gel. To excite the resonances, the frequency of the electric field was swept by using the variable-frequency internal oscillator of the wave analyzer as described in section II (see Figure 2). The output from the amplifier was monitored on an oscilloscope to check that there was no phase shift in the signal due to the amplification and connection to the cell. The output signal from the photodiode was fed into the wave analyzer (Figure 2) and compared to the driving signal. The resulting response (due to the resonant deformation induced birefringence) was then plotted as a function of the frequency.

As described in section II, the cell was rectangular and thus the transverse modes are plane waves with eigenfrequencies that depend on the boundary conditions. For the gel used in obtaining the data shown in Figure 3, the gel

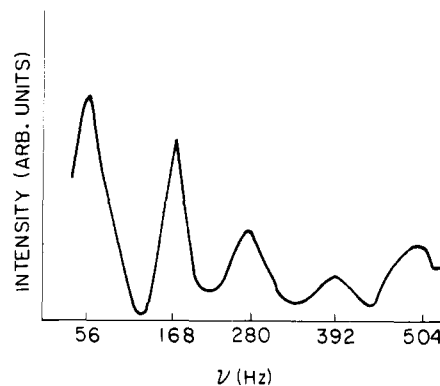


Figure 4. Resonance scan for a ~ 0.7 wt % poly(diacetylene) gel. The boundary conditions were zero displacement at one wall and zero velocity at the other. Therefore, only odd harmonics are observed.

surface was in contact with both electrodes, implying rigid boundary conditions. Hence the resonant acoustic modes correspond to multiple half-wavelengths in the cell with nodes at the electrodes, and the eigenfrequencies are (see eq 19 with $q_n = 2\pi n/2d$)

$$\nu_n = \omega_0(q_n)/2\pi = nv_s/2d \quad (20)$$

where d is the spacing between the two electrodes which form the boundaries. Indeed Figure 3 shows equally separated resonances which can be fit to eq 20 giving $v_s = 33$ cm s⁻¹. This implies a shear modulus, $\mu = \rho v_s^2 \approx 980$ dyn/cm², which is consistent with that obtained independently¹⁰ with the torsion resonator method for a gel of similar concentration.

A different result, for a stiffer gel, is shown in Figure 4, where the boundary conditions were changed. The gel was pulled carefully away from one of the electrodes in order to maintain the smoothness of the surface. In this situation we expect only odd harmonics (the free surface is an antinode); thus the eigenfrequencies are

$$\nu_n = (2n + 1)v_s/4d \quad (21)$$

Note that the difference in frequencies between two consecutive resonances is 112 Hz whereas $\nu_0 = 56$ Hz, half of that difference. The sound velocity is therefore $v_s \approx 67$ cm/s ($\mu \approx 4500$ dyn/cm²). Details on the concentration dependence of μ are summarized in section VI, where the results obtained from three different techniques are included.

V. Transient Decay of Underdamped Gel Modes

In sections III and IV we discussed the resonant coupling of a sinusoidal alternating electric field to the transverse acoustic modes of the gel. More generally, the gel will respond such that the deformation (and hence the birefringence) will be a superposition of harmonic modes with eigenfrequencies which depend on the boundary conditions. For example, after the external force is abruptly turned off, the gel is expected to relax toward equilibrium through all available routes (both underdamped and overdamped) with amplitudes that depend on the geometry and boundary conditions, etc. The birefringence technique described in section II will detect the decaying deformation during this relaxation. We therefore expect that subsequent to an abrupt step decrease in the external field, the birefringence signal (Δn) will decrease as (see section II)

$$I(t) = (I_0 \sin 2\beta) \sum A_n \exp(-t/\tau_n) \quad (22)$$

where n runs over all the possible modes and A_n are the relative amplitudes by which the gel deformation will

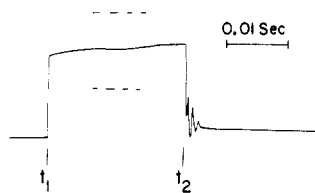


Figure 5. Typical transient decay of the deformation-induced gel birefringence signal. The two dashed lines indicate the ac level on top of the dc response (see section V).

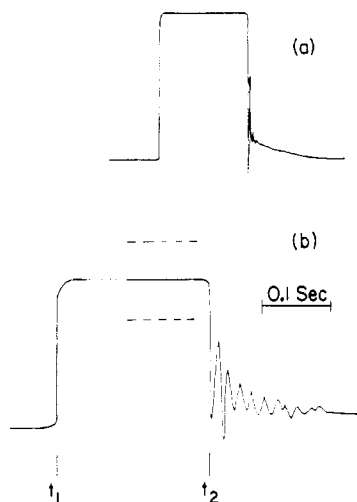


Figure 6. Transient decay of the deformation-induced birefringence for a gel with relatively high concentration, ~0.5 wt %; the time scale in (b) is magnified by a factor of 10 relative to (a). The electric field was applied at time t_1 , and it was switched off at t_2 . The two dashed lines denote the ac part on top of the average response (see section V).

decay. The corresponding complex relaxation "times" τ_n are given by

$$\tau_n^{-1} = \tau_0^{-1} \pm ((\tau_0^{-1})^2 - \omega_0^2(q_n))^{1/2} \quad (23)$$

For the transverse modes discussed in the previous sections, $\tau_0 \approx 2\rho/\eta$ (see eq 19). For the underdamped modes, $\omega_n > \tau_0^{-1}$ so that the decay would be oscillatory with an envelope which decays as $\exp(-t/\tau_0)$, where $\tau_0 \sim 0.1$ – 1 s, for η in the range 1–10 P.

On the other hand, the overdamped modes will decay monotonically. As analyzed in detail by Tanaka, Hocker, and Benedek,¹⁶ the characteristic decay (for modes in which the network and solvent displacements are not in phase) will be $\tau^{-1} = 1/2[K + (4/3)\mu]/\phi$.

Figure 5 shows a clear demonstration of the decaying oscillatory motion due to the underdamped modes. Starting at an initial time t , the gel was driven at a frequency much higher than its fundamental frequency, typically 400–500 Hz. The two dashed lines represent the ac signal on top of the average (nonresonant) dc birefringence. At a later time, t_2 , the high-frequency driving field was switched off (typical switching time was $<10^{-3}$ s). The initial fall-off is very rapid, after which one observes a series of more slowly decaying oscillations (decay time of the order of a few milliseconds).

In the context of eq 22 and 23 (and the resonance data of the previous section), we associate the decaying oscillations with the longest wavelength modes, since they are the narrowest (longest lifetime) and the easiest to excite. We can therefore extract the fundamental frequency of the gel from the period of the oscillations. Although higher harmonic content is evident, interference between the various modes (see eq 22) makes a more detailed analysis (including the harmonics) somewhat difficult. The de-

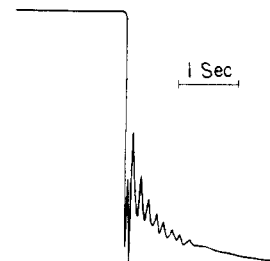


Figure 7. Decay of the birefringence of a gel with concentration just above c_0 ; the fundamental mode frequency is $\nu_0 = 6$ Hz, corresponding to a sound velocity of only 6 cm s^{-1} .

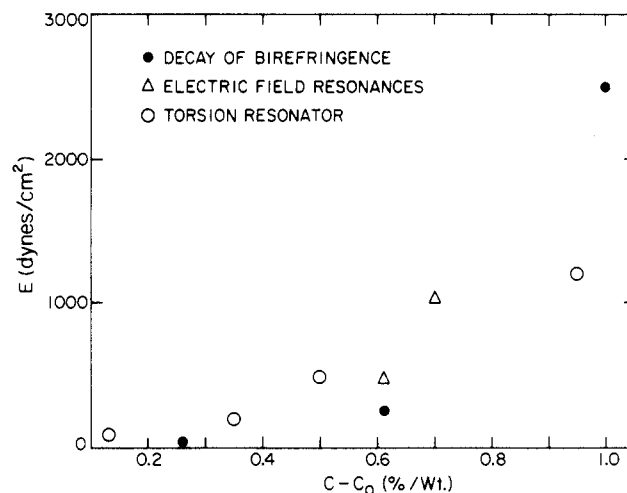


Figure 8. Collection of all the data available on poly(diacetylene)-4BCMU gels from all three methods. For the torsion resonator results, see ref 10.

caying oscillations thus provide an independent method for direct measurement of the elastic properties of the gel. Moreover, the existence of underdamped free oscillations unambiguously confirms the resonance mode interpretation of the data shown in Figures 3 and 4.

Figure 6 shows the data obtained from a gel with polymer concentration similar to that of Figure 2. The fundamental frequency is ~50 Hz (in good agreement with the data of Figure 2) and the decay time is of the order of 50 ms. This method is extremely sensitive, and typically we found that it could be used for measurements closer to the critical concentration than the resonance method. Figure 7 shows the lowest frequency (closest concentration to c_0) that we detected: ~6 Hz. This implies a shear modulus of $\mu \sim 35 \text{ dyn/cm}^2$, corresponding to a remarkably slow wave sound velocity, $v_s \approx 6 \text{ cm s}^{-1}$.

VI. Concentration Dependence of the Shear Modulus of the Poly(diacetylene)-4BCMU/Toluene Gel: Summary and Conclusion

We have presented data from two independent and novel methods which allowed us to study the elastic properties of this highly polarizable gel. Sinclair et al.¹⁰ used a torsion resonator method to measure the shear modulus of the same gel at several polymer (network) concentrations. Although the methods of measurement are very different, the absolute values of the shear modulus obtained by Sinclair et al.¹⁰ are very close to the results obtained with the electrooptic birefringence techniques developed in this paper.

Shear modulus data obtained from all three techniques are plotted vs. $(c - c_0)$ in Figure 8. Although there is considerable scatter, the data define a smooth nonlinear dependence of the shear modulus. Since the concentra-

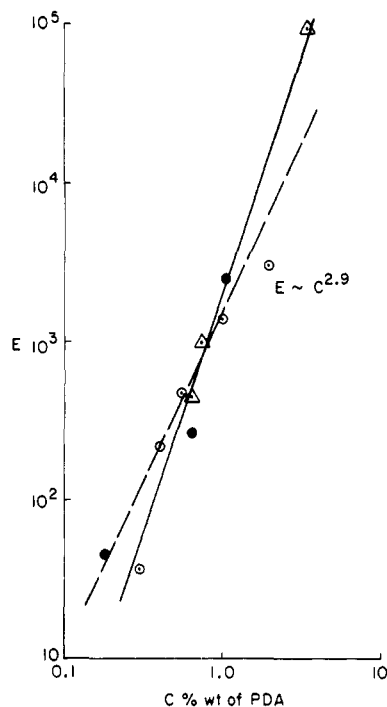


Figure 9. log-log plot of the data presented in Figure 8, including a very stiff gel investigated by the resonance method. The solid line is the best fit through all the points and indicates a power law dependence, $E \propto c^{2.9}$. The dashed line depicts the c^2 dependence which is discussed in the text (see section III).

tions span a range well beyond the critical regime ($(c - c_0) \ll c_0$) we examine the overall dependence of $\mu(c)$ via the log-log plot of Figure 9. The values for μ span more than 3 orders of magnitude. The solid line is a least-squares fit to a power law dependence; the slope implies $\mu \sim c^{2.9}$. Note that although Sinclair et al. obtained a power law of 1.7 on a $(c - c_0)$ plot, their data are quite consistent with this steeper $\mu(c)$ dependence.

The theory developed in section III predicted a c^2 dependence for $\mu(c)$. The results collected on Figure 9 are however more compatible with a higher power law. We note, however, that the prediction of a c^2 dependence assumed rigid joints and zero temperature. Since the intermolecular forces (hydrogen bonding and van der Waals) are relatively weak, some joint flexibility is surely to be expected. Since the effect of joint flexibility would be to decrease the total rigidity, we expect that for low c , $\mu \sim c^x$, with $x \geq 2$ (the lower bound of 2 is fixed by the arguments in section III).

Since the data were obtained at (or above) room temperature, some contribution from the entropy to the elasticity is to be expected. However, Sinclair et al.¹⁰ found that the gel rigidity decreases linearly with temperature, whereas an entropic contribution to the elasticity would

increase linearly with temperature. Two possible explanations are to be considered:

(i) The proximity of the rod-coil transition implies the possibility of a temperature-dependent Young's modulus for rod bending.

(ii) The content of the infinite network is not constant with temperature; molecules leave the infinite network and dilute it.

Although these additional complications have not been included in a detailed analysis, we conclude that the poly(diacetylene)-4BCMU/toluene gel has elastic properties which are a consequence of it being an infinite network of rigid rods with semirigid joints at finite temperatures.

Acknowledgment. The research reported in this paper was supported by the National Science Foundation, Grant DMR83-12725.

Registry No. Poly(diacetylene)-4BCMU (homopolymer), 68777-93-5; poly(diacetylene)-4BCMU (SRU), 100082-23-3.

References and Notes

- (1) Patel, G. N.; Chance, R. R.; Witt, J. D. *J. Chem. Phys.* **1979**, *70*, 4387.
- (2) Chance, R. R.; Patel, G. N.; Witt, J. D. *J. Chem. Phys.* **1979**, *71*, 206.
- (3) Lim, K. C.; Fincher, C. R.; Heeger, A. J. *Phys. Rev. Lett.* **1983**, *50*, 1934.
- (4) Lim, K. C.; Heeger, A. J. *J. Chem. Phys.* **1985**, *82*, 522.
- (5) Lim, K. C.; Kapitulnik, A.; Zacher, R.; Heeger, A. J. *J. Chem. Phys.* **1985**, *82*, 516.
- (6) See, e.g.: de Gennes, P.-G. "The Physics of Liquid Crystals"; Oxford University Press: London, 1974; Chapter 2.
- (7) Doi, M.; Edwards, S. F. *J. Chem. Soc., Faraday Trans. 2* **1978**, *74*, 560.
- (8) Doi, M.; Kuzuu, N. Y. *J. Polym. Sci., Polym. Phys. Ed.* **1980**, *18*, 409.
- (9) See, e.g.: de Gennes, P.-G. "Scaling Concepts in Polymer Physics"; Cornell University Press: Ithaca, NY, 1979; Chapter V.
- (10) Sinclair, M.; Lim, K. C.; Heeger, A. J. *Phys. Rev. Lett.* **1983**, *51*, 1768. In this paper the data were presented as f_0^2 (proportional to E), where f_0 is the resonance frequency of the torsion oscillator. The values quoted in the text are the actual values for E obtained by Sinclair et al., including all the geometrical factors.
- (11) Plachetta, C.; Rau, N. O.; Hanck, A.; Schulz, R. C. *Makromol. Chem., Rapid Commun.* **1982**, *3*, 249.
- (12) Casalnuovo, S.; Heeger, A. J. *Phys. Rev. Lett.* **1985**, *53*, 2254.
- (13) The nematic phase of such a gel should be very much like a regular nematic phase. In particular, we expect quite a high jump at the isotropic-to-nematic transition. This is in contrast to what was found experimentally in ref 12. A possible scenario that will eventually cause a nearly isotropic gel with small nematic order is when the polymers will have highly anisotropic interaction that favors the molecules to be perpendicular when attached to each other.
- (14) Kapitulnik, A.; Casalnuovo, S. A.; Lim, K. C.; Heeger, A. J. *Phys. Rev. Lett.* **1985**, *53*, 469.
- (15) See, e.g.: Stoylov, S. P. *Adv. Colloid Interface Sci.* **1971**, *3*, 45.
- (16) Tanaka, T.; Hocker, L. O.; Benedek, G. B. *J. Chem. Phys.* **1973**, *59*, 5151.